Density-functional calculations of prefactors and activation energies for H diffusion in $BaZrO_3$

Per G. Sundell, Mårten E. Björketun, and Göran Wahnström
Department of Applied Physics, Chalmers University of Technology, S-412 96 Göteborg, Sweden
(Received 15 June 2007; published 27 September 2007)

Density-functional calculations are used to investigate hydrogen diffusion in the solid-state proton conductor $BaZrO_3$. Activation energies and prefactors for the rate of proton transfer and reorientation are evaluated for a defect-free region of this simple cubic perovskite-structured oxide. Both semiclassical over-barrier jumps and phonon-assisted tunneling transitions between sites are considered. It is found that the classical barriers for the elementary transfer and reorientation steps are both of the order of 0.2 eV. The quantum-mechanical zero-point motion effects are found to be sizable, to effectively reduce the barrier heights, and to make the prefactors similar for the transfer and reorientation steps. The Flynn-Stoneham model [Phys. Rev. B **1**, 3966 (1970)] of phonon-assisted tunneling yields an activation energy of around 0.2 eV and a very small prefactor for proton transfer, whereas the corresponding adiabatic model gives a similar activation energy but a much larger prefactor. It is suggested that the effect of other defects such as dopants has to be included for a proper description of hydrogen diffusion in this material.

DOI: 10.1103/PhysRevB.76.094301 PACS number(s): 66.30.Dn, 66.35.+a, 71.15.Mb

I. INTRODUCTION

Many perovskite-structured oxides exhibit significant proton conductivity at elevated temperatures[1] and are potential candidates for use in a wide range of electrochemical applications.[2] From a more fundamental point of view, these materials are also interesting as model systems for fast protonic transport in solids.[3] Experimentally, the mobility of protonic defects in oxides is usually found to decrease with decreasing temperatures following an Arrhenius behavior,[4] with activation energies and prefactors that are mainly consistent with a semiclassical description of hydrogen hopping between neighboring oxygen sites in the lattice.[5] Nevertheless, for a light interstitial such as H, diffusion can be expected to take place primarily via a quantum-mechanical tunneling mechanism at sufficiently low temperatures.[6,7] Indeed, the dielectric relaxation data for hydrated $BaNd_xCe_{1-x}O_3$, $x=0.05$, by Kuskovsky *et al.*[8] show a transition to a near temperature-independent rate for $T \lesssim 85$ K that was interpreted as a tunneling process.

Several theoretical studies have previously addressed the preferred sites, transition states, and conduction pathways for hydrogen impurities in various perovskite oxides using first-principles calculations with a static lattice[9–14] or a molecular-dynamics[15–18] approach. However, neither of these takes directly the quantum nature of the motion of the light hydrogen atom into account. For instance, using embedded cluster Hartree-Fock-type calculations, Cherry *et al.*[9,10] investigated proton transfer between two neighboring oxygen atoms in $LaAlO_3$. They found a very low classical activation barrier for this process and suggested that proton transfer may take place via a "barrierless" or nonclassical (tunneling) mechanism where fluctuations of the surrounding lattice are required to produce a configuration where the environments of two neighboring oxygens become equivalent before proton transfer can occur. It has also been suggested[19–21] that the "small-polaron" theories of phonon-assisted hopping[22–24]—which have been widely used to interpret the anomalous isotope dependence of the diffusion coefficient for hydrogen in bcc metals at low temperatures[25–27]—might be applicable for H in perovskites, but so far no direct evaluation of the activation energies from first principles has been attempted.

In the present work, we have used density-functional calculations to investigate classical (over-barrier) and quantum (tunneling) diffusion of protonic defects in a perovskite-structured oxide. Activation energies and prefactors are given for the two elementary migration steps, O-H$\cdots$O transfer and O-H reorientation, in a defect-free region of cubic $BaZrO_3$. Particular emphasis is placed on the role of lattice relaxations and vibrational properties of the system.

II. METHODS

A. Basic formalism

We will consider the hopping of a hydrogen atom between two adjacent interstitial sites separated by a potential energy barrier. In the regime of purely over-barrier motion, a simple transition state theory (TST)[28] expression for the hop rate ν is

$$\nu = \frac{k_B T}{h}\frac{Z^{\ddagger}}{Z}, \tag{1}$$

where k_B is the Boltzmann constant, h is Planck's constant, and Z and $Z^{\ddagger}$ denote the classical partition functions of the initial and transition states, respectively. Within a harmonic approximation, the vibrational properties of the solid can be expressed in terms of the N normal modes $\{\hbar\omega_i\}_{i=1}^{N}$ of the system at the potential minimum and the $(N-1)$ normal modes $\{\hbar\omega_i^{\ddagger}\}_{i=1}^{N-1}$ at the saddle point. Equation (1) then predicts an Arrhenius behavior for the hop rate,[29]

$$\nu = \nu_0^{\mathrm{cl}} e^{-\Delta E/k_B T}, \tag{2}$$

where the activation energy ΔE is equal to the classical *migration barrier* V_m, i.e., the difference in potential energy between the saddle-point and minimum configurations, and the prefactor

$$\nu_0^{\mathrm{cl}} = \frac{1}{2\pi} \frac{\prod_{i=1}^{N} \omega_i}{\prod_{i=1}^{N-1} \omega_i^{\ddagger}} \tag{3}$$

is often interpreted as a characteristic "attempt frequency." Due to the small reduced mass of a protonic defect, the vibrational energy levels become discrete and widely spaced. As discussed by Kehr,[30] a simple modification of the TST that includes this effect can be obtained by replacing the classical partition functions in Eq. (1) by their quantum-mechanical analog. The activation energy is then be given by

$$\Delta E = V_m + \frac{1}{2}\sum_{i=1}^{N-1} \hbar\omega_i^{\ddagger} - \frac{1}{2}\sum_{i=1}^{N} \hbar\omega_i, \tag{4}$$

which is a sum of the classical migration barrier and a vibrational zero-point energy (ZPE) correction, whereas the prefactor becomes

$$\nu_0^{\mathrm{qm}} = \frac{k_B T}{h} \frac{\prod_{i=1}^{N} (1 - e^{-\hbar\omega_i/k_B T})}{\prod_{i=1}^{N-1} (1 - e^{-\hbar\omega_i^{\ddagger}/k_B T})}. \tag{5}$$

In the limit of high temperatures ($k_B T \gg \hbar\omega$), Eq. (5) reduces to the classical result of Eq. (3), whereas at low temperatures ($k_B T \ll \hbar\omega$), a general prefactor $k_B T/h$ appears that is independent of isotope mass and host lattice properties.

A hydrogen may also tunnel quantum mechanically through the barriers separating adjacent sites. For a light interstitial coupled to the vibrational modes of the host lattice, the Flynn-Stoneham model[23] of phonon-assisted hopping predicts a thermally activated hop rate,

$$\nu = \left(\frac{\pi}{4\hbar^2 E_c k_B T}\right)^{1/2} J_0^2 e^{-E_c/k_B T}. \tag{6}$$

Here, J_0 is the "bare" tunneling matrix element for hydrogen and E_c is the so-called *coincidence energy*; it is the energy required to bring the relaxed host lattice into a configuration where the hydrogen levels on the two neighboring sites become equivalent and tunneling can take place. The use of Eq. (6) requires that the temperature is sufficiently high that many phonons are excited. The Flynn-Stoneham model is based on a nonadiabatic picture, i.e., the probability for tunneling is small during the time scale for coincidence. On the other hand, if the tunneling probability is large, an adiabatic picture is more relevant. The hop rate is then given by[31]

$$\nu = \nu_D e^{-E_a/k_B T}, \tag{7}$$

where the activation energy E_a becomes similar to the classical barrier height adjusted for the ZPE and the prefactor ν_D is related to the inverse period of the lattice vibrations. At lower temperatures, lattice vibrations are frozen out, and the diffusion of hydrogen would take place predominantly via a zero-phonon tunneling mechanism which gives a much weaker temperature dependence for the hop rate compared with the thermally activated behavior predicted by Eqs. (2), (6), and (7).[31]

B. Computational details

Our density-functional calculations are performed using the plane-wave pseudopotential method as implemented in the Vienna *ab initio* simulation package (VASP).[32,33] For the exchange-correlation functional, we use a generalized gradient approximation (GGA) due to Wang and Perdew.[34] Such functionals are known to describe hydrogen bond strengths with an accuracy comparable to that of explicitly correlated quantum chemistry techniques,[35] although the accuracy for proton transfer barriers has been questioned.[36] The electron-ion interaction is described by the projector augmented wave method.[37] A plane-wave basis set with a cutoff energy of 400 eV was used in all calculations. Brillouin zone sampling was performed using a $6\times6\times6$ k-point grid for the five-atom primitive cell. This gives an equilibrium lattice constant a_0=4.25 Å for pure $BaZrO_3$ in good agreement with experimental data.[38]

Hydrogen interstitials were introduced in periodically repeated supercells consisting of $2\times2\times2$ or $3\times3\times3$ primitive cells with the number of k points in each direction reduced accordingly. This corresponds to a hydrogen concentration $c=1/8$ and $c=1/27$, respectively. To simulate the presence of hydrogen in the +1 charge state (H^+), an electron was removed from the hydrogen loaded supercells and the resulting electronic charge was neutralized by the standard means of including a uniform "jellium" background.[39] Structural optimizations were performed at constant volume until all residual forces were smaller than 0.05 eV/Å. Vibrational frequencies for protonic defects in various fixed lattice configurations were calculated within a harmonic approximation by evaluating and diagonalizing a dynamical matrix using the smaller supercell. All calculations in the present study were performed non-spin-polarized.

III. RESULTS AND DISCUSSION

A. Stable sites and migration paths

For a hydrogen atom in the +1 charge state, the equilibrium position in $BaZrO_3$ is close to an oxide ion, with the O-H distance equal to 0.98 Å and with the O-H axis oriented along the bisector of two oxygen-oxygen connecting lines. There are thus four equivalent interstitial sites around each oxygen in the lattice, as shown in Fig. 1. Similar configurations of protonic defects have been found in several different perovskite oxides, both experimentally[40] and theoretically.[9,10,13,14] The hydrogen interstitial interacts strongly with the host lattice, which results in a pronounced displacement of the equilibrium positions of the surrounding atoms (see Fig. 1). Correspondingly, the localization or "self-trapping" energy (defined as the change in total energy V_{st} associated with allowing the host lattice to relax around an interstitial at the stable site) is large for H in $BaZrO_3$: We find $V_{\mathrm{st}}=-1.14$ eV (−0.90 eV) for $c=1/27$ ($c=1/8$). Due to the strong lattice polarization and deformation of the ionic

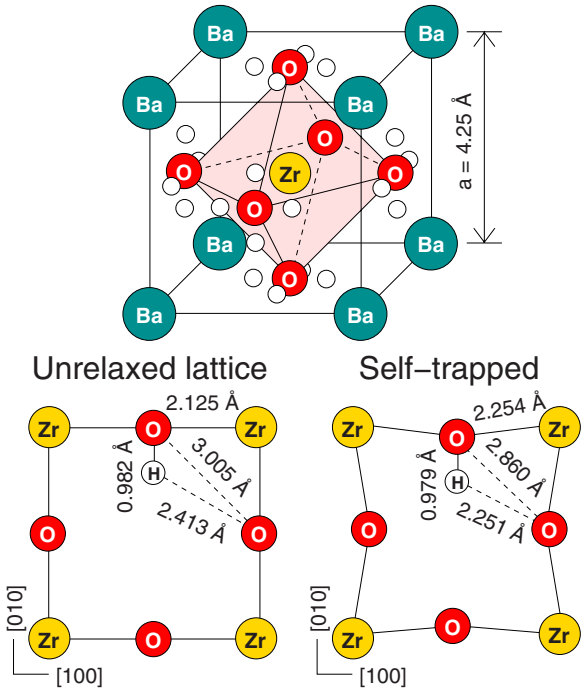

FIG. 1. (Color online) The equilibrium position for a hydrogen interstitial in $BaZrO_3$ (calculated lattice parameter a_0=4.25 Å) is close to an oxide ion, with the O-H distance equal to 0.98 Å and the O-H axis oriented along the bisector of two oxygen-oxygen connecting lines. The protonic defect interacts strongly with the host lattice, which is manifested as a large self-trapping distortion of the positions of the surrounding atoms.

$BaZrO_3$ crystal, this is considerably larger than the self-trapping energies previously obtained for hydrogen/metal systems, which are around −0.19 eV for H in bulk Nb and Ta (Ref. 41) and only −0.03 eV for H on a Cu surface.[42]

To investigate the local motion of a self-trapped protonic defect, we have calculated the harmonic frequencies of vibration for a hydrogen atom at the stable site with the host lattice ions held rigidly in their relaxed positions. This gives a high-frequency O-H stretch mode $\hbar\omega_1$=435 meV and two lower frequency O-H wag modes $\hbar\omega_2$=110 meV and $\hbar\omega_3$ =75 meV. The calculated frequencies are consistent with infrared spectroscopy data, which typically show a broad absorption band around in the range 2500–3500 cm^{-1} (corresponding to $\hbar\omega$=310–430 meV) for hydrated acceptor-doped $BaZrO_3$.[43]

The long-range protonic transport in perovskite oxides occurs via a so-called Grotthuss mechanism, consisting of a sequence of O-H···O transfers (transitions between sites coordinated to different oxygens) and O-H reorientations (transitions between different sites coordinated to the same oxygen).[3] As a consequence of the high symmetry of the cubic $BaZrO_3$ lattice, all protonic sites in a dopant-free region of the material have the same energy (see Fig. 1). Moreover, all transfer and reorientation barriers are symmetric and mutually equivalent. Determining the potential energy along the preferred protonic pathway thus reduces to mapping out one barrier of each kind.

TABLE I. Classical transfer and reorientation barriers calculated for hydrogen in a fixed and in a fully relaxed $BaZrO_3$ lattice using two different supercells corresponding to a defect concentration c =1/27 (c=1/8).

	V_m (eV)			
Barrier	Fixed lattice		Relaxed lattice	
Transfer	1.27	(1.29)	0.21	(0.22)
Reorientation	0.33	(0.33)	0.18	(0.17)

B. Over-barrier motion

We first consider proton migration via an over-barrier mechanism. Two different saddle-point configurations, corresponding to proton transfer and reorientation, have been investigated. These were determined by restricting the hydrogen position to a plane perpendicular to the path connecting the initial and final states, while relaxing the remaining ionic coordinates of the supercell. At the transition state of the transfer step, the proton is located at the center of a slightly bent O···H···O configuration. The initial O-H bond is markedly elongated to 1.23 Å, whereas the O···O separation contracts to 2.42 Å. These results are in good agreement with previous molecular-dynamics simulations,[17] indicating that proton transfer is facilitated via the formation of transient hydrogen bonds.[3] For the transition state of the reorientation step, we instead find that the O-H bond is contracted to 0.97 Å, whereas the O···O separation increases to 2.99 Å (which is close to the corresponding distance in the unperturbed lattice; see Fig. 1).

The classical migration barriers can be calculated as the difference in total energy of the system when the proton is at a saddle point and when the proton is self-trapped. These energy differences are given in Table I. It is seen that the transfer barrier is slightly higher than the reorientation barrier and that both barriers appear well converged with respect to the supercell size. These results clearly demonstrate the importance of taking lattice relaxations into account, as discussed by Kreuer.[3] Previously calculated values of the migration barriers in $BaZrO_3$ show a significant variation: Münch *et al.* found a transfer barrier equal to 0.69 eV from a static calculation[16] and 0.83±0.65 eV from a molecular-dynamics simulation,[17] both based on a "tight-binding" density-functional theory (DFT) approach. In more recent studies, Shi *et al.*[13] found a transfer barrier equal to 0.37 eV close to a dopant atom in In-doped $BaZrO_3$, whereas Gomez *et al.*[14] reported a transfer barrier of 0.25 eV and a reorientation barrier of 0.14 eV without dopant. Both these studies include lattice relaxations, and the latter results are in good agreement with our findings in the present work.

The vibrational frequencies of a protonic defect drastically change as the system approaches either of the transition states. At the saddle point of the transfer step, we find for hydrogen two real modes at 210 and 170 meV and one imaginary (unstable) mode at 125i meV. It is the high-frequency O-H stretch mode that gradually softens and becomes unstable. As can be expected for a strongly hydrogen-

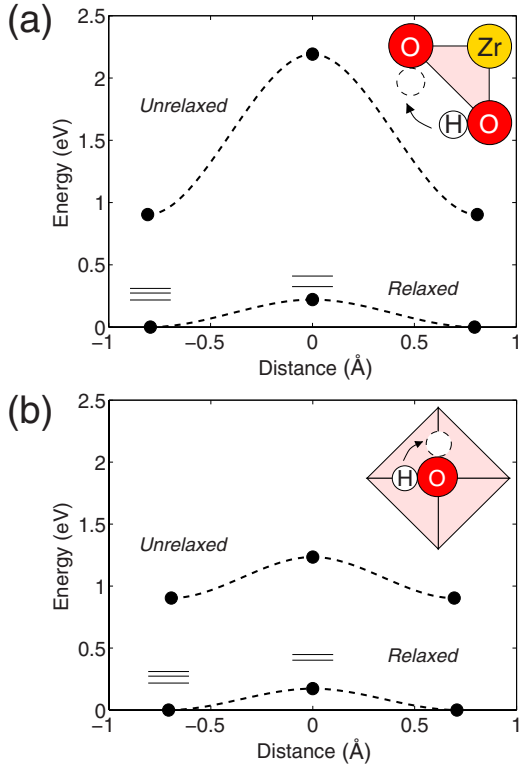

FIG. 2. (Color online) Schematic illustration of (a) over-barrier O-H···O transfer and (b) O-H reorientation in $BaZrO_3$. Filled circles indicate data obtained from DFT calculations, whereas the dashed lines are a guide for the eye that illustrate the total-energy variation for different positions of the hydrogen in a relaxed and an unrelaxed lattice, respectively. Vibrational excitation energies $\hbar\omega$ for the proton at various positions are also indicated.

bonded configuration,[44] this is accompanied by a significant hardening of the wag modes. At the saddle point of the reorientation step, we instead find two real modes at 460 and 90 meV and one imaginary (unstable) mode at 70*i* meV. Here, it is one of the O-H wag modes that becomes unstable, accompanied by a slight hardening of the stretch mode and a corresponding softening of the remaining wag mode. In Fig. 2, we show the total-energy variation and vibrational energy levels for a hydrogen at different positions in a host lattice in the unrelaxed, self-trapped, and saddle-point configurations.

The semiclassical activation energies ΔE for proton transfer and reorientation are evaluated using Eq. (4) and adding to the classical migration barriers given in Table I the difference in vibrational ZPE between the transition states and the self-trapped state. The latter quantities are given in Table II. In the simplest approximation, only the H frequencies are assumed to change during a transition, while all other atomic frequencies remain unaffected. This gives a negative contribution and would lower the migration barriers for proton transfer and reorientation by −0.12 and −0.04 eV, respectively. For reorientation, the ZPE correction roughly corresponds to the energy of the missing wag mode, whereas for transfer, the correction is considerably smaller than the energy of the missing stretch mode as a consequence of the large change in the remaining modes. Although these very

TABLE II. Over-barrier proton transfer and reorientation in cubic $BaZrO_3$: Quantum-mechanical zero-point energy corrections to the migration barriers ΔZPE, corresponding prefactors ν_0^{qm} calculated at $T=300$ K and $T=600$ K, and the purely classical prefactors ν_0^{cl} valid in the high-temperature limit.

Process	ΔZPE (eV)	ν_0^{qm} (ps^{-1}) $T=300$ K	ν_0^{qm} (ps^{-1}) $T=600$ K	ν_0^{cl} (ps^{-1})
Transfer	−0.12	5.8	8.9	24.8
Reorientation	−0.04	6.0	10.2	20.9

low barriers (~0.1 eV for both proton transfer and reorientation) are consistent with the observation of a rapid localized motion for protonic defects in perovskite oxides,[45] they are significantly smaller than the activation energies typically obtained from conductivity measurements (0.43–0.50 eV depending on the choice of dopant).[46] This might be due to a tendency of standard DFT approaches to underestimate proton transfer barriers. In particular, test calculations on small model systems have shown that the barrier height given by ordinary GGA functionals is of the order of 0.10–0.15 eV lower than that given by more sophisticated quantum chemistry techniques.[36] However, another explanation would be that protons are "trapped" near dopant atoms in the material as suggested from muon spin relaxation and quasielastic neutron scattering experiments by Hempelmann *et al.*[40,45,47] The observed activation energies would then be roughly equal to the sum of the migration barriers in the "free" state (investigated in the present work) and an additional energy required to form mobile protons (which may amount to a few tenths of an eV based on the DFT results of Islam *et al.*[12,18] for various zirconates). A more accurate treatment would require that the proton barriers are mapped out in the vicinity of dopant atoms.[48]

The calculated prefactors of proton transfer and reorientation are given in Table II. At very high temperatures, the classical limit becomes valid and the prefactors can be estimated using ν_0^{cl} as given by Eq. (3). For the reorientation step, this gives an effective frequency that roughly corresponds to the missing wag mode (~0.1 eV or 25 ps^{-1}), but for the transfer step, the result is considerably smaller than that of the missing stretch mode (~0.4 eV or 100 ps^{-1}). The latter is a direct consequence of the hardening of the O-H wag modes that occur for the strongly hydrogen-bonded saddle-point configuration. Finally, both prefactors decrease with decreasing temperatures, which can be seen by taking energy discretization into account and using the more general ν_0^{qm} as given by Eq. (5).

C. Quantum tunneling

We next consider proton transfer by a tunneling mechanism. The Arrhenius parameters of the hop rate may then deviate significantly from the classical or semiclassical behavior.[31]

Due to the self-trapping lattice distortion, periodicity is destroyed so that if the hydrogen is moved to a neighboring

site, without allowing the lattice to readjust, the total energy of the system would be higher (see Fig. 2). The nearest-neighbor site energies thus become shifted by $V_{nn}=1.04$ eV (0.87 eV) for $c=1/27$ ($c=1/8$). At zero temperature, this large asymmetry effectively prohibits tunneling between the sites. However, at finite temperatures, thermal fluctuations of the lattice may occasionally produce a configuration where the sites become equivalent and a transition may take place.

In the *adiabatic picture*, the lowest symmetric configuration of this kind can be obtained by freezing the lattice at the classical saddle-point geometry (O···O separation of 2.42 Å as discussed in Sec. III B) and then optimizing the proton position at one of the two neighboring oxide ions.[9,10] This results in an elongation of the initial O-H bond to 1.07 Å. The energy needed to form this equivalence environment—where the proton can easily tunnel between the two oxide ions—from the self-trapped state is $V_a=0.19$ eV (0.19 eV) for $c=1/27$ ($c=1/8$). This value is only slightly less, 0.02 eV (0.03 eV), than the classical migration barrier V_m. We note that Cherry *et al.*[9,10] have previously estimated this quantity for $LaAlO_3$ from a combination of first-principles calculations and atomistic simulations, but they obtained a value of 0.69 eV, which is considerably larger than what we find for $BaZrO_3$. Furthermore, the ZPE corrections should be comparable to those of the over-barrier hopping. Thus, the activation energy E_a in Eq. (7) is close to the semiclassical ΔE (see Sec. III B) and will have a similar, pronounced, isotope dependence. The prefactor ν_D, on the other hand, is expected to be essentially isotope independent.[31] It can be approximated with the frequency of the O-Zr-O bending mode, which is of the order of 6 ps^{-1} in $BaZrO_3$,[49,50] and is hence similar to the prefactor ν_0^{qm} obtained for the protonic over-barrier hopping.

In the *nonadiabatic picture*, the equivalence configuration can be determined by using a weighted sum of forces when relaxing the ions, as discussed elsewhere.[51] In the resulting geometry, the initial O-H bond is slightly elongated to 1.03 Å, whereas the O···O separation contracts to 2.59 Å. The energy required to create this "coincidence" configuration from the self-trapped state is $V_c=0.19$ eV (0.17 eV) for $c=1/27$ ($c=1/8$). This is considerably larger than for hydrogen in metals [for instance, the coincidence energy is only around 0.02 eV for H in Nb and Ta (Refs. 41 and 51) and 0.01 eV for H on a Cu surface (Refs. 42 and 51)], indicating a strong coupling to the lattice for the diffusing proton. Moreover, the ratio V_c/V_{nn} is smaller than the 1/4 expected for a purely harmonic lattice.[52] This indicates a slight anharmonicity, which may be due to the strong lattice coupling and the correspondingly large ionic displacements involved in the transfer process. Tomoyose *et al.*[21] have previously reported an activation energy for phonon-assisted tunneling equal to 0.56 eV using a model calculation for a general cubic perovskite oxide. We note that this result is also considerably larger than the coincidence energy obtained for hydrogen in $BaZrO_3$ in the present study.

In Fig. 3, we show the total-energy variation as a function of the hydrogen position for the self-trapped and coincidence configurations of the host lattice. The harmonic frequencies of vibration for H in the coincidence configuration are quite

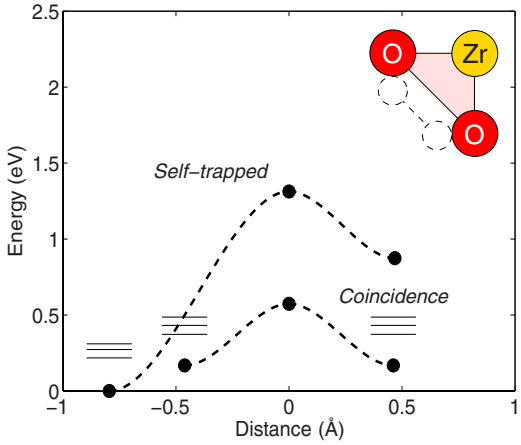

FIG. 3. (Color online) Schematic illustration of phonon-assisted tunneling via a symmetric coincidence configuration for hydrogen in $BaZrO_3$. Filled circles indicate total energies obtained from DFT calculations, whereas the dashed lines are a guide for the eye. Vibrational excitation energies $\hbar\omega$ for the proton at various positions are also indicated.

similar to the H frequencies in the self-trapped state, which means that ZPE corrections will only give a small contribution to the activation energy in Eq. (6) and thus $E_c \approx V_c$. To determine the prefactor, we must also calculate the tunneling splitting for hydrogen in the symmetric potential of the coincidence configuration. A simple one-dimensional Wentzel-Kramers-Brillouin estimate is

$$J_0 = \left(\frac{\hbar\omega}{2\pi}\right)\exp\left\{-\frac{1}{\hbar}\int_{-x0}^{+x0}\sqrt{2m[v(x)-E]}dx\right\}, \qquad (8)$$

where m is the particle mass, E its energy, ω the vibrational frequency at the potential minimum, and the turning points $\pm x_0$ defined by $v(\pm x_0)=E$. We approximate $v(x)$ by a smooth interpolation of the remaining barrier for hydrogen in the coincidence configuration (which has a width of 0.92 Å and a height of 0.41 eV; see Fig. 3) and take the three-dimensional character of the problem into account by setting $E=1/2\hbar\omega$=the difference in ZPE when hydrogen is at the potential minimum and when it is at the barrier top (around 0.13 and 0.09 eV for H and D, respectively). Numerical quadrature of the integral in Eq. (8) gives $J_0=0.3$ (0.9×10^{-2}) meV for H (D). Due to these narrow tunneling matrix elements, the preexponential factor in Eq. (6) is several orders of magnitude smaller than the TST prefactors and, in addition, highly isotope dependent.

IV. SUMMARY AND CONCLUSIONS

To summarize, we have used density-functional calculations to determine the prefactors and activation energies for H^+ diffusion in a defect-free region of a perovskite-structured oxide. In the highly symmetric $BaZrO_3$ system, there are only two different migration barriers for a hydrogen interstitial, corresponding to the elementary O-H···O transfer and O-H reorientation steps.[3]

We first consider a purely classical diffusion mechanism. Although our calculated barriers (0.21 and 0.18 eV for proton transfer and reorientation, respectively) are in general agreement with previous theoretical DFT results,[14,17] they are at least a factor 2 smaller than the activation energies obtained experimentally from conductivity data.[46] Based on a quantum-mechanically modified TST that takes into account that the vibrational levels of light interstitials are discrete and widely separated,[30] the temperature dependence of the jump rates is investigated in some detail. We find that quantum effects imply considerably smaller prefactors than what is expected from a purely classical rate theory at realistic temperatures ($T=300-600$ K). We also find that the results are quite similar for the two different processes, the transfer and reorientation steps. This is a consequence of a strongly hydrogen-bonded transition state for the proton transfer step, which increases the frequencies of the remaining modes and gives a prefactor that is approximately an order of magnitude smaller than the anticipated frequency of the missing O-H stretch mode. For the activation energies, we find a negative vibrational ZPE contribution that tends to lower both migration barriers even further. While this is consistent with the rapid localized motion that has been observed experimentally for protonic defects in perovskite oxides,[45] it also suggests that the long-range protonic transport in these materials is not rate limited by the elementary transfer and reorientation steps (in defect-free regions), but rather by some other mechanism such as trapping diffusion.[40,45,47]

Another interesting aspect is the possibility of tunneling. Within the Flynn-Stoneham model[23] for phonon-assisted tunneling in $BaZrO_3$, we find an activation energy of 0.19 eV that is significantly larger than that for H in metals.[41,42,51] Since, in addition, the hydrogen tunneling matrix elements are found to be small, it is likely that the Flynn-Stoneham model[23] for hydrogen diffusion can be excluded in the present system. Instead, the adiabatic picture of thermally activated tunneling appears to be more relevant. This model gives a prefactor and an isotope dependent activation energy very similar to those obtained for the over-barrier hopping mechanism. It might therefore be difficult to experimentally distinguish between these two processes.

In conclusion, we find barriers for the elementary transfer and reorientation steps of proton migration in defect-free regions of $BaZrO_3$ to be considerably less than what is found experimentally from conductivity data. Although an uncertainty is associated with the use of DFT, and too low barriers can be obtained using standard generalized gradient approximations,[36] this effect seems to be too small to solely account for the discrepancy between our calculated migration barriers and measured activation energies. Therefore, we argue that the effect of other defects, such as dopants, has to be included to get a proper description of proton diffusion. Furthermore, the quantum-mechanical zero-point motion effects are found to be sizable, effectively reduce the barrier heights, and make the prefactors similar for the transfer and reorientation steps. Quasielastic neutron scattering studies of the proton motion in the present model system would be highly desirable.[53,54]

ACKNOWLEDGMENTS

This work was supported by the National Graduate Schools in Scientific Computing and Material Science and by the Foundation for Strategic Research via the ATOMICS program, Sweden. Allocations of computer resources through the Swedish National Allocation Committee are gratefully acknowledged.

[1] H. Iwahara, T. Esaka, H. Uchida, and N. Maeda, Solid State Ionics **3-4**, 359 (1981).
[2] H. Iwahara, in *Proton Conductors: Solids, Membranes and Gels-Materials and Devices*, edited by P. Colomban (Cambridge University Press, Cambridge, 1992), Chap. 8.
[3] K. D. Kreuer, Chem. Mater. **8**, 610 (1996).
[4] T. Norby, Solid State Ionics **40/41**, 857 (1990).
[5] A. S. Nowick and A. V. Vaysleyb, Solid State Ionics **97**, 17 (1997).
[6] R. P. Bell, *The Tunnel Effect in Chemistry* (Chapman and Hall, London, 1980).
[7] V. I. Gol'danskii, L. I. Trakhtenberg, and V. N. Fleurov, *Tunneling Phenomena in Chemical Physics* (Gordon and Breach, New York, 1989).
[8] I. Kuskovsky, B. S. Lim, and A. S. Nowick, Phys. Rev. B **60**, R3713 (1999).
[9] M. Cherry, M. S. Islam, J. D. Gale, and C. R. A. Catlow, Solid State Ionics **77**, 207 (1995).
[10] M. Cherry, M. S. Islam, J. D. Gale, and C. R. A. Catlow, J. Phys. Chem. **99**, 14614 (1995).
[11] F. Shimojo, K. Hoshino, and H. Okazaki, J. Phys. Soc. Jpn. **65**, 1143 (1996).
[12] M. S. Islam, P. R. Slater, J. R. Tolchard, and T. Dinges, Dalton Trans. **19**, 3061 (2004).
[13] C. Shi, M. Yoshino, and M. Morinaga, Solid State Ionics **176**, 1091 (2005).
[14] M. A. Gomez, M. A. Griffin, S. Jindal, K. D. Rule, and V. R. Cooper, J. Chem. Phys. **123**, 094703 (2005).
[15] F. Shimojo, K. Hoshino, and H. Okazaki, J. Phys. Soc. Jpn. **66**, 8 (1997).
[16] W. Münch, G. Seifert, K. D. Kreuer, and J. Maier, Solid State Ionics **97**, 39 (1997).
[17] W. Münch, K. D. Kreuer, G. Seifert, and J. Maier, Solid State Ionics **136**, 183 (2000).
[18] M. S. Islam, R. A. Davies, and J. D. Gale, Chem. Mater. **13**, 2049 (2001).
[19] A. L. Samgin, Solid State Ionics **136-137**, 291 (2000).
[20] E. Matsushita, Solid State Ionics **145**, 445 (2001).
[21] T. Tomoyose, N. Shimoji, and K. Wakamura, J. Phys. Soc. Jpn. **74**, 3011 (2005).
[22] T. Holstein, Ann. Phys. (N.Y.) **8**, 343 (1959).
[23] C. P. Flynn and A. M. Stoneham, Phys. Rev. B **1**, 3966 (1970).
[24] Y. Kagan and M. I. Klinger, J. Phys. C **7**, 2791 (1974).
[25] D. Emin, M. I. Baskes, and W. D. Wilson, Phys. Rev. Lett. **42**,

791 (1979).
[26] A. Klamt and H. Teichler, Phys. Status Solidi B **134**, 533 (1986).
[27] H. R. Schober and A. M. Stoneham, Phys. Rev. Lett. **60**, 2307 (1988).
[28] H. Eyring, J. Chem. Phys. **3**, 107 (1935).
[29] G. H. Vineyard, J. Phys. Chem. Solids **3**, 121 (1957).
[30] K. W. Kehr, in *Hydrogen in Metals I: Basic Properties*, Topics in Applied Physics, Vol. 28, edited by G. Alefeld and J. Völkl (Springer-Verlag, Berlin, 1978), Chap. 8.
[31] Y. Fukai, *The Metal-Hydrogen System* (Springer-Verlag, Berlin, 1993).
[32] G. Kresse and J. Hafner, Phys. Rev. B **47**, 558 (1993).
[33] G. Kresse and J. Furthmüller, Phys. Rev. B **54**, 11169 (1996).
[34] Y. Wang and J. P. Perdew, Phys. Rev. B **44**, 13298 (1991).
[35] J. Ireta, J. Neugebauer, and M. Scheffler, J. Phys. Chem. A **108**, 5692 (2004).
[36] V. Barone and C. Adamo, J. Chem. Phys. **105**, 11007 (1996).
[37] P. E. Blöchl, Phys. Rev. B **50**, 17953 (1994).
[38] *Landolt-Börnstein: Numerical Data and Functional Relationships in Science and Technology*, edited by K.-H. Hellwege and A. M. Hellwege, New Series, Group III, Vol. 7E (Springer-Verlag, Berlin, 1977).
[39] J. Lento, J.-L. Mozos, and R. M. Nieminen, J. Phys.: Condens. Matter **14**, 2637 (2002).
[40] R. Hempelmann, M. Soetratmo, O. Hartmann, and R. Wäppling, Solid State Ionics **107**, 269 (1998).
[41] P. G. Sundell and G. Wahnström, Phys. Rev. B **70**, 224301 (2004).
[42] P. G. Sundell and G. Wahnström, Phys. Rev. B **70**, 081403(R) (2004).
[43] M. Karlsson, M. E. Björketun, P. G. Sundell, A. Matic, G. Wahnström, D. Engberg, L. Börjesson, I. Ahmed, S. Eriksson, and P. Berastegui, Phys. Rev. B **72**, 094303 (2005).
[44] A. Novak, in *Structure and Bonding* (Springer, Berlin, 1974), Vol. 18, pp. 177–212.
[45] T. Matzke, U. Stimming, C. Kramonik, M. Soetratmo, R. Hempelmann, and F. Güthoff, Solid State Ionics **86-88**, 621 (1996).
[46] K. D. Kreuer, S. Adams, W. Münch, A. Fuchs, U. Klock, and J. Maier, Solid State Ionics **145**, 295 (2001).
[47] R. Hempelmann, C. Karmonik, T. Matzke, M. Cappadonia, U. Stimming, T. Springer, and M. A. Adams, Solid State Ionics **77**, 152 (1995).
[48] M. E. Björketun, P. G. Sundell, and G. Wahnström, Phys. Rev. B **76**, 054307 (2007).
[49] P. G. Sundell, M. E. Björketun, and G. Wahnström, Phys. Rev. B **73**, 104112 (2006).
[50] C. H. Perry, D. J. McCarthy, and G. Rupprecht, Phys. Rev. **138**, A1537 (1965).
[51] P. G. Sundell and G. Wahnström, Phys. Rev. Lett. **92**, 155901 (2004).
[52] H. Grabert and H. R. Schober, in *Hydrogen in Metals III: Properties and Applications*, Topics in Applied Physics, Vol. 73, edited by H. Wipf (Springer-Verlag, Berlin, 1997), Chap. 2.
[53] D. Wilmer, K. D. Kreuer, and B. Frick, iLL Experimental Report No. 7-07-204, 2004.
[54] M. Karlsson, D. Engberg, M. E. Björketun, A. Matic, L. Börjesson, P. G. Sundell, G. Wahnström, I. Ahmed, S.-G. Eriksson, P. Berastegui, B. Farago, and P. Falus (unpublished).